Mean Curvature Flow of Closed Curves Evolving in Two Dimensional Manifolds

Miroslav Kolář[a], Daniel Ševčovič[b,*]

[a]Department of Mathematics, Faculty of Nuclear Sciences and Physical Engineering Czech Technical University in Prague, Trojanova 13, Prague, 12000, Czech Republic
[b]Comenius University Bratislava, Department of Applied Mathematics and Statistics, Faculty of Mathematics, Physics and Informatics, Comenius University in Bratislava, Mlynska dolina, 842 48 Bratislava, Slovakia

Abstract

We investigate the motion of a family of closed curves evolving on an embedded or immersed manifold in three dimensional Euclidean space according to the geometric evolution law. We derive a system of nonlinear parabolic equations describing the motion of curves belonging to a given two-dimensional manifold. We consider both embedded and immersed manifolds. Using the abstract theory of analytic semiflows, we prove the local existence, uniqueness of Hölder smooth solutions to the governing system of nonlinear parabolic equations for the position vector parametrization of evolving curves. We apply the method of flowing finite volumes in combination with the methods of lines for numerical approximation of the governing equations. Numerical experiments support the analytical conclusions and demonstrate the efficiency of the method.

Keywords: Curvature-driven flow, binormal flow, analytic semi-flows, Hölder smooth solutions, flowing finite-volume method.

1. Introduction

In this article we investigate motion of a family $\{\Gamma_t, t \geq 0\}$ of closed curves evolving in three dimensional Euclidean space (3D) according to the geometric evolution law:

$$\partial_t \mathbf{X} = v_N \mathbf{N} + v_B \mathbf{B} + v_T \mathbf{T}, \tag{1}$$

where the unit tangent $\mathbf{T}$, normal $\mathbf{N}$ and binormal $\mathbf{B}$ vectors form moing Frenet frame. In this paper, we restrict our interest to the investigation of the dynamics of three-dimensional closed curves on embedded manifolds.

The three-dimensional motion of closed curves is motivated by various physical applications arising in materials sciences, fluid dynamics, or molecular biology. In fluid dynamics, the motion of the curve space is often applied to the analysis of vortex structures firstly studied by Helmholtz [21]. For a detailed summary of recent advances in this field, we refer the reader to Kolář, Beneš and Ševčovič [7] and references therein. In that paper, we investigated the dynamics of vortex

*Corresponding author
Email addresses: kolarmir@fjfi.cvut.cz (Miroslav Kolář), sevcovic@fmph.uniba.sk (Daniel Ševčovič)

rings represented by interacting space curves. However, vortex-ring dynamics generally does not deal with knotted curves.

In material sciences, more particularly in dislocation dynamics, a geodesic description of space curves has recently been used in Kolář *et al.* [28] as a convenient mathematical framework to simulate a dislocation cross-slip phenomenon in the crystalline structure of solids. Moreover, the dynamics of dislocations climb [38, 39] investigated by Niu *et al.* motivates us to study the problem of diffusion and transport along a moving space curve, as we investigated in Beneš *et al.* [8]. In nanomaterials manufacturing, a procedure called electrospinning, i.e. jetting polymer solutions in high electric fields into ultrafine nanofibers, is frequently used - see, e.g., Reneker [42], Yarin *et al.* [17], He *et al.* [20] and particular references therein. Structures arising from the electrospinning procedure move in space according to (1) and under the effect of electric forces [47] to form nanofibers. In molecular biology, three-dimensional structures moving in space according to (1) under the effect of chemical kinetics are observed. Such structures can interact with each other. See, e.g. Shlomovitz [45, 46] or Fierling [14], Kang [24] or Glagolev [18]. Recently, a motion in the normal and binormal directions of a system of space curves bound together via a Biot-Savart type of force from the local existence and uniqueness point of view has been discussed by Kolář and Ševčovič in [29]. In [27], the flow that preserves the area was treated by geodesic description of the curves. The computational aspects of the Lagrangian description of space curves have been elaborated by Narayananin and Beneš in [37]. Structure of constrained gradient flows of planar curves hs been recently studied by Kemmochi, Miyatake, and Sakakibara in [25].

In a recent paper [11], Deckelnick and Nürnberg introduced an innovative approach to the evolution of parametric curves influenced by the anisotropic curve shortening flow, as presented in $\mathbb{R}^3$. This formulation is contingent upon meticulous adjustment of the tangential velocity within the parameterization, thus reformulating the problem into a strictly parabolic differential equation. The equation is expressed in divergence form, which facilitates the formulation of a natural variational numerical method. Optimal error estimates are derived for a fully discrete finite element model utilizing piecewise linear elements. Numerical experiments support the analytical conclusions and demonstrate the efficiency of the method. In [9] by Binz, optimal error estimates for semidiscrete and fully discrete approximations describing isotropic curve shortening flow are also studied in three dimensions.

The paper is organized as follows. In the second section, a parametric description of evolving curves is introduced. In the third section, we restrict our interest to the motion on a closed surface without boundary. We derive a force term that attaches the curve to the surface and formulate the system of governing equations for such a restricted 3D motion. In the fourth section, we discuss the conditions for the existence and uniqueness of classical Hölder solutions. We also recall the role of the tangential velocity when using the parametric description. In the fifth section, we propose the numerical approximation scheme based on the flowing finite-volume approach. Finally, several computational examples are presented in the sixth section.

2. Lagrangian description of evolving curves

Our methodology for solving (1) is based on the so-called direct Lagrangian approach investigated by Dziuk [12], Deckelnick [10], Gage and Hamilton [15], Mikula and Ševčovič [33, 34, 35, 36], and references therein). We explore the direct Lagrangian approach for an analytical and numerical solution of the geometric motion law (1). The evolving family of curves Γ_t is parametrized by the mapping $\mathbf{X}$ such that $\Gamma_t = \{\mathbf{X}(u,t), u \in I, t \geq 0\}$ where $\mathbf{X} : I \times [0,\infty) \to \mathbb{R}^3$ is a smooth mapping.

In what follows, we denote by $I = \mathbb{R}/\mathbb{Z} \simeq S^1$ the periodic interval $I = [0,1]$ isomorphic to the unit circle S^1. We assume that the scalar velocities v_N, v_T, v_B are smooth functions of the position vector $\mathbf{X} \in \mathbb{R}^3$, the curvature κ, the torsion τ, that is,

$$v_K = v_K(\mathbf{X}, \kappa, \tau, \mathbf{T}, \mathbf{N}, \mathbf{B}, \Gamma), \quad K \in \{T, N, B\}.$$

The unit tangent vector $\mathbf{T}$ to Γ_t is defined as $\mathbf{T} = \partial_s \mathbf{X}$, where s is the unit arc-length parametrization defined by $ds = |\partial_u \mathbf{X}| du$. Here, $|\mathbf{x}|$ and $\mathbf{x}^\intercal \mathbf{y} \equiv \mathbf{x} \cdot \mathbf{y}$ denote the Euclidean norm and the inner product of the vectors $\mathbf{x}, \mathbf{y} \in \mathbb{R}^d$. The curvature κ of a curve Γ_t is defined as $\kappa = |\partial_s \mathbf{X} \times \partial_s^2 \mathbf{X}| = |\partial_s^2 \mathbf{X}|$. If $\kappa > 0$, we can define the Frenet frame along the curve Γ_t with unit normal $\mathbf{N} = \kappa^{-1} \partial_s^2 \mathbf{X}$ and binormal vectors $\mathbf{B} = \mathbf{T} \times \mathbf{N}$, respectively. Recall the Frenet-Serret formulae:

$$\frac{\mathrm{d}}{\mathrm{d}s} \begin{pmatrix} \mathbf{T} \\ \mathbf{N} \\ \mathbf{B} \end{pmatrix} = \begin{pmatrix} 0 & \kappa & 0 \\ -\kappa & 0 & \tau \\ 0 & -\tau & 0 \end{pmatrix} \begin{pmatrix} \mathbf{T} \\ \mathbf{N} \\ \mathbf{B} \end{pmatrix},$$

where τ is the torsion of Γ given by $\tau = \kappa^{-2} (\mathbf{T} \times \partial_s \mathbf{T})^\intercal \partial_s^2 \mathbf{T} = \kappa^{-2} (\partial_s \mathbf{X} \times \partial_s^2 \mathbf{X})^\intercal \partial_s^3 \mathbf{X}$. We study a coupled system of evolutionary equations describing evolution of closed 3D curves evolving in normal and binormal directions,

More specifically, we focus on the motion of a family of curves evolving in 3D and satisfying the geometric law

$$\partial_t \mathbf{X} = a \partial_s^2 \mathbf{X} + \mathbf{F}(\mathbf{X}, \partial_s \mathbf{X}) + \alpha \partial_s \mathbf{X}, \tag{2}$$

where $a = a(\mathbf{X}, \mathbf{T}) > 0$, and $\mathbf{F} = \mathbf{F}(\mathbf{X}, \mathbf{T})$ are bounded and smooth functions of their arguments. Since $\partial_s^2 \mathbf{X} = \kappa \mathbf{N}$ and $\mathbf{B} = \mathbf{T} \times \mathbf{N}$ the relationship between geometric equations (1) and (2) reads as follows:

$$v_N = a\,\kappa + \mathbf{F}^\intercal \mathbf{N}, \quad v_B = \mathbf{F}^\intercal \mathbf{B}, \quad v_T = \mathbf{F}^\intercal \mathbf{T} + \alpha. \tag{3}$$

The system of equations (2) is subject to the initial condition

$$\mathbf{X}(u, 0) = \mathbf{X}_0(u), u \in I = \mathbb{R}/\mathbb{Z} \simeq S^1, \tag{4}$$

representing parametrization of the initial curve Γ_0.

3. Evolution of closed curves on a closed surface without boundary

In this section, we analyze the evolution of closed curves on a two-dimensional surface without boundary. First, we discuss the evolution of curves in embedded manifolds.

3.1. Evolution of curves on embedded manifolds

Assume $\mathscr{M} \in \mathbb{R}^3$ is an embedded manifold given by $\mathscr{M} = \{\mathbf{X} = (X_1, X_2, X_3)^\intercal \in \mathbb{R}^3,\ f(\mathbf{X}) = 0\}$ where $f(\mathbf{X}) : \mathbb{R}^3 \to \mathbb{R}$ is a C^3 smooth regular map. This means that $\nabla f(\mathbf{X}) \neq 0$ for $\mathbf{X} \in \mathscr{M}$.

Let $\phi(u,t) = f(\mathbf{X}(u,t))$. Then

$$\begin{aligned} \partial_t \phi &= \nabla f(\mathbf{X})^\intercal \partial_t \mathbf{X} \\ &= \nabla f(\mathbf{X})^\intercal \left(a \partial_s^2 \mathbf{X} + \mathbf{F} + \alpha \partial_s \mathbf{X} \right) = a \nabla f(\mathbf{X})^\intercal \partial_s^2 \mathbf{X} + \nabla f(\mathbf{X})^\intercal \mathbf{F} + \alpha \nabla f(\mathbf{X})^\intercal \partial_s \mathbf{X} \\ &= a \partial_s \left(\nabla f(\mathbf{X})^\intercal \partial_s \mathbf{X} \right) - a \partial_s \mathbf{X}^\intercal \nabla^2 f(\mathbf{X}) \partial_s \mathbf{X} + \nabla f(\mathbf{X})^\intercal \mathbf{F} + \alpha \partial_s \phi \\ &= a \partial_s^2 \phi - a \partial_s \mathbf{X}^\intercal \nabla^2 f(\mathbf{X}) \partial_s \mathbf{X} + \nabla f(\mathbf{X})^\intercal \mathbf{F} + \alpha \partial_s \phi \end{aligned}$$

because $\partial_s \phi = \nabla f(\mathbf{X})^\intercal \partial_s \mathbf{X}$.

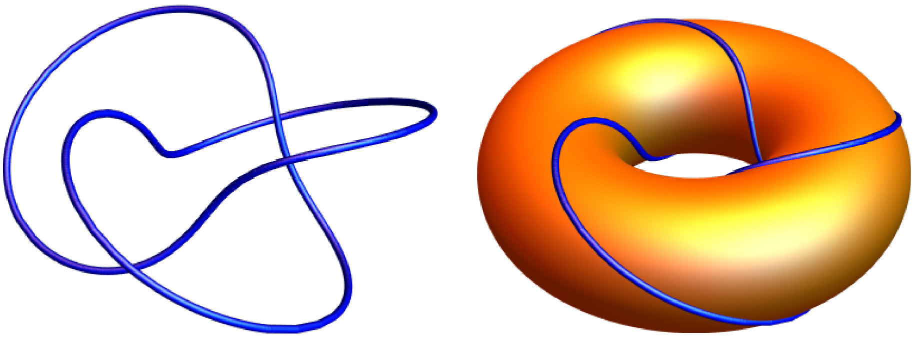

a) b)

Figure 1: A knotted curve a) belonging to the embedded torus surface b).

Theorem 1. *Suppose that the external force* $\mathbf{F}$ *is given by*

$$\mathbf{F}(\mathbf{X}, \mathbf{T}) = a \frac{\mathbf{T}^\intercal \nabla^2 f(\mathbf{X}) \mathbf{T} + h(f(\mathbf{X}))}{|\nabla f(\mathbf{X})|^2} \nabla f(\mathbf{X}) \tag{5}$$

where $h : \mathbb{R} \to \mathbb{R}$ *is a smooth function,* $h(0) = 0$*. If the initial curve* $\Gamma_0 \subset \mathscr{M}$ *then the evolving family curves* Γ_t*, for* $t > 0$*, belong to the manifold* $\mathscr{M} = \{\mathbf{X} \in \mathbb{R}^3,\ f(\mathbf{X}) = 0\}$*. Furthermore, the tangential velocity* $v_T = \alpha$*.*

Proof. If the initial curve $\Gamma_0 \subset \mathscr{M}$ then $\phi(\cdot, 0) = f(\mathbf{X}(\cdot, 0)) = 0$. The function ϕ is a solution to the parabolic equation:

$$\partial_t \phi = a \partial_s^2 \phi + h(\phi) + \alpha \partial_s \phi, \qquad . \tag{6}$$

with a zero initial condition $\phi(\cdot, 0) = 0$. Since $h(0) = 0$ we have $\phi(\cdot, t) = 0$ for all $t > 0$. That is $\Gamma_t \subset \mathscr{M}$. The projection of $\mathbf{F}^\intercal \mathbf{T}$ to the tangent direction is vanishing. In fact, as $0 = \partial_s \phi = \nabla f(\mathbf{X})^\intercal \mathbf{T}$. we have $\mathbf{F}(\mathbf{X}, \mathbf{T})^\intercal \mathbf{T} = a \frac{\mathbf{T}^\intercal \nabla^2 f(\mathbf{X}) \mathbf{T} + h(f(\mathbf{X}))}{|\nabla f(\mathbf{X})|^2} \nabla f(\mathbf{X})^\intercal \mathbf{T} = 0$.

□

Next, we shall prove that a closed curve $\bar{\Gamma} \subset \mathscr{M}$ is locally asymptotically stable in the sense that $\phi(\cdot, t) = f(\mathbf{X}(\cdot, t)) \to 0 \equiv f(\bar{\mathbf{X}}(\cdot))$ as $t \to \infty$.

Proposition 1. *Suppose that* $h : \mathbb{R} \to \mathbb{R}$ *is a smooth function such that* $h(0) = 0,\ h'(0) < 0$*, and that the closed curve* $\bar{\Gamma} \subset \mathscr{M}$*. Then there exists* $\delta > 0$ *such that* $\|\phi(\cdot, t)\|_2 = O(\exp(-\omega_0 t))$*, as* $t \to \infty$*, provided that* $\|\phi(\cdot, 0)\|_2 \le \delta$ *where* $\phi(\cdot, t) = f(\mathbf{X}(\cdot, t))$ *for a closed curve* $\Gamma_t = \{\mathbf{X}(u, t),\ u \in I\}$*.*

Proof. Suppose that the curve $\bar{\Gamma} = \{\bar{\mathbf{X}}(u), u \in I\} \subset \mathscr{M}$ is uniformly parameterized, i.e., $\bar{g}(u) = L(\bar{\Gamma})$ for all $u \in I$ where $\bar{g}(u) = |\partial_u \bar{\mathbf{X}}(u)|$. Without the loss of generality, we may assume that $\alpha \equiv 0$ and

$$\partial_t \phi = \mathscr{L} \phi \tag{7}$$

where $\mathscr{L}$ is the linearization of equation (6) at $\bar{\phi} = f(\bar{\mathbf{X}}) \equiv 0$, i.e., $\mathscr{L} \phi = \frac{\bar{a}(u)}{\bar{g}(u)^2} \frac{\partial^2 \phi}{\partial u^2} + h'(0) \phi$. Since $h'(0) < 0$, the real part of the spectrum $\sigma(\mathscr{L})$ is strictly negative, that is, $\mathcal{R}e\, \sigma(\mathscr{L}) \le h'(0) < 0$. As a consequence, $\|\phi(\cdot, t)\|_2 = O(\exp(-\omega_0 t))$, as $t \to \infty$. Here $\|\phi(\cdot, t)\|_2^2 = \int_0^1 \phi(u, t)^2 du$ and $h'(0) < \omega_0 < 0$. Applying the principle of linearized stability of scalar semilinear parabolic equations (cf. Henry [22]), we conclude the existence of a $\delta > 0$ neighborhood of $\bar{\varphi} \equiv 0$ such that $\|\phi(\cdot,t)\|_2 = O(\exp(-\omega_0 t))$, as $t \to \infty$, provided that $\|\phi(\cdot,0)\|_2 \le \delta$. Because $\phi = f(\mathbf{X})$, the proof of the proposition follows.

□

Theorem 2. *Suppose that the external force* $\mathbf{F}$ *is defined by equation (5), and the initial curve* $\Gamma_0 \subset \mathscr{M}$. *Then the geometric flow of the curves, which satisfies the law (2), represents the length-shortening flow on the surface* $\mathcal{M}$, *i.e.,* $\frac{d}{dt}L(\Gamma_t) \le 0$, *where* $L(\Gamma_t)$ *denotes the total length of the curve* Γ_t.

Proof. Suppose that the initial curve $\Gamma_0 \subset \mathscr{M}$. With regard to Theorem 1 we have $\Gamma_t \subset \mathscr{M}$ for any $t \ge 0$. That is, $\phi(s,t) \equiv f(\mathbf{X}(s,t)) = 0$ for all $s \in [0, L(\Gamma_t)]$ and $t \ge 0$. Hence $0 = \partial_s \phi = \nabla f(\mathbf{X})^\intercal \mathbf{T}$, and

$$0 = \partial_s^2 \phi = \mathbf{T}^\intercal \nabla^2 f(\mathbf{X}) \mathbf{T} + \nabla f(\mathbf{X})^\intercal \partial_s \mathbf{T} = \mathbf{T}^\intercal \nabla^2 f(\mathbf{X}) \mathbf{T} + \kappa \nabla f(\mathbf{X})^\intercal \mathbf{N}.$$

The projection of the velocity $\partial_t \mathbf{X}$ to the normal direction $\mathbf{N}$ is given by

$$\begin{aligned} v_N &= (a\,\partial_s^2 \mathbf{X} + \mathbf{F})^\intercal \mathbf{N} = a\,\kappa + a\,\frac{\mathbf{T}^\intercal \nabla^2 f(\mathbf{X}) \mathbf{T}}{|\nabla f(\mathbf{X})|^2} \nabla f(\mathbf{X})^\intercal \mathbf{N} = a\,\kappa - a\,\kappa \frac{(\nabla f(\mathbf{X})^\intercal \mathbf{N})^2}{|\nabla f(\mathbf{X})|^2} \\ &= a\,\kappa - a\,\kappa \frac{(\nabla f(\mathbf{X})^\intercal \mathbf{N})^2}{|\nabla f(\mathbf{X})|^2} = a\,\kappa \frac{(\nabla f(\mathbf{X})^\intercal \mathbf{B})^2}{|\nabla f(\mathbf{X})|^2} \end{aligned} \tag{8}$$

because $|\nabla f(\mathbf{X})|^2 = (\nabla f(\mathbf{X})^\intercal \mathbf{N})^2 + (\nabla f(\mathbf{X})^\intercal \mathbf{T})^2 + (\nabla f(\mathbf{X})^\intercal \mathbf{B})^2 = (\nabla f(\mathbf{X})^\intercal \mathbf{N})^2 + (\nabla f(\mathbf{X})^\intercal \mathbf{B})^2$.

$$\frac{d}{dt} L(\Gamma_t) = -\int_{\Gamma_t} \kappa v_N ds = -\int_{\Gamma_t} a\,\kappa^2 \frac{(\nabla f(\mathbf{X})^\intercal \mathbf{B})^2}{|\nabla f(\mathbf{X})|^2} ds \le 0. \tag{9}$$

□

Remark 1. *The geodesic curvature* κ^g *of a curve* $\Gamma \subset \mathcal{M}$ *can be defined as a projection of the derivative* $\partial_s \mathbf{T}$ *to the unit vector* $\mathbf{N}^g$ *perpendicular to* $\mathbf{T}$ *and belonging to the tangent space* $T_X(\mathcal{M})$ *at the point* $\mathbf{X} \in \mathcal{M}$. *Both vectors belong to the tangent space* $T_X(\mathcal{M})$ *that is perpendicular to the outer normal vector* $\nabla f(\mathbf{X})$ *to the surface* $\mathcal{M}$. *The unit normal vector to the surface* $\mathcal{M}$ *is given by the vector* $\nabla f(\mathbf{X})/|\nabla f(\mathbf{X})|$. *Therefore,* $\mathbf{N}^g = (\nabla f(\mathbf{X}) \times \mathbf{T})/|\nabla f(\mathbf{X})|$. *Hence,*

$$\begin{aligned} \kappa^g &= \partial_s \mathbf{T}^\intercal \mathbf{N}^g = \kappa \mathbf{N}^\intercal \mathbf{N}^g = \kappa \mathbf{N}^\intercal (\nabla f(\mathbf{X}) \times \mathbf{T})/|\nabla f(\mathbf{X})| \\ &= \kappa \nabla f(\mathbf{X})^\intercal (\mathbf{T} \times \mathbf{N})/|\nabla f(\mathbf{X})| = \kappa (\nabla f(\mathbf{X})^\intercal \mathbf{B})/|\nabla f(\mathbf{X})|. \end{aligned}$$

According to Mikula and Ševčovič [36, Eq. (12)] we have $\frac{d}{dt}L(\Gamma_t) = -\int_{\Gamma_t} \kappa^g v_{N^g} ds$. *If the normal velocity* v_{N^g} *is proportional to the geodesic curvature,* $v^{N^g} = a\kappa^g$ *then we obtain*

$$\frac{d}{dt} L(\Gamma_t) = -\int_{\Gamma_t} \kappa^g v_{N^g} ds = -\int_{\Gamma_t} a(\kappa^g)^2 ds = -\int_{\Gamma_t} a\,\kappa^2 \frac{(\nabla f(\mathbf{X})^\intercal \mathbf{B})^2}{|\nabla f(\mathbf{X})|^2} ds \le 0. \tag{10}$$

which is the relation (9).

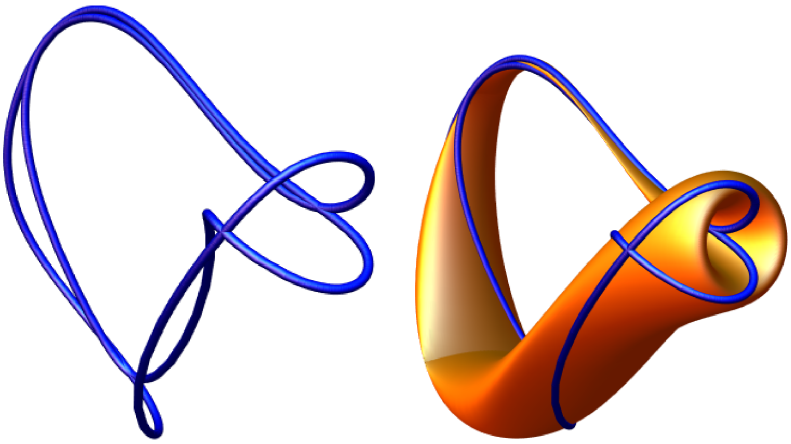

a) b)

Figure 2: a) An initial knotted curve belonging to the Klein bottle immersed surface b)

3.2. Evolution of curves on immersed manifolds

In this section, we discuss the evolution of 3D curves evolving on immersed manifolds. We consider an immersed manifold $\mathcal{M} = \{\mathbf{X} = \mathcal{X}(\mathbf{Y}), \quad \mathbf{Y} \in I \times I\}$ where $\mathbf{Y} = (Y_1, Y_2)^\intercal$ and $\mathbf{X} = (X_1, X_2, X_3)^\intercal$ are parameterized by immersion $\mathcal{X} : I \times I \to \mathbb{R}^3$. Here we remind the reader that $I = [0, 1]$ is the 1-periodic interval. Then

$$\partial_t \mathbf{X} = \nabla\mathcal{X}(\mathbf{Y})^\intercal \partial_t \mathbf{Y}, \qquad \partial_s \mathbf{X} = \nabla\mathcal{X}(\mathbf{Y})^\intercal \partial_s \mathbf{Y}, \qquad \partial_s^2 \mathbf{X} = \nabla\mathcal{X}(\mathbf{Y})^\intercal \partial_s^2 \mathbf{Y} + \partial_s \mathbf{Y}^\intercal \nabla^2 \mathcal{X}(\mathbf{Y}) \partial_s \mathbf{Y}$$

where $\nabla\mathcal{X} = \nabla\mathcal{X}(\mathbf{Y})$ is the 2×3 matrix:

$$\nabla\mathcal{X} = \begin{pmatrix} \frac{\partial \mathcal{X}_1}{\partial Y_1} & \frac{\partial \mathcal{X}_2}{\partial Y_1} & \frac{\partial \mathcal{X}_3}{\partial Y_1} \\ \frac{\partial \mathcal{X}_1}{\partial Y_2} & \frac{\partial \mathcal{X}_2}{\partial Y_2} & \frac{\partial \mathcal{X}_3}{\partial Y_2} \end{pmatrix},$$

and, the vector $\partial_s \mathbf{Y}^\intercal \nabla^2 \mathcal{X}(\mathbf{Y}) \partial_s \mathbf{Y} \in \mathbb{R}^3$ is constructed as follows:

$$\partial_s \mathbf{Y}^\intercal \nabla^2 \mathcal{X}(\mathbf{Y}) \partial_s \mathbf{Y} = (\partial_s \mathbf{Y}^\intercal \nabla^2 \mathcal{X}_k(\mathbf{Y}) \partial_s \mathbf{Y})_{k=1,2,3} \in \mathbb{R}^3, \quad \nabla^2 \mathcal{X}_k = \left(\frac{\partial^2 \mathcal{X}_k}{\partial Y_i \partial Y_j} \right)_{i,j=1,2}.$$

The 2×3 matrix $\nabla\mathcal{X}(\mathbf{Y})$ has the full rank equal to 2 because the mapping $\mathcal{X}$ is assumed to be an immersion. Furthermore, as $\mathbf{X} = \mathcal{X}(\mathbf{Y})$ we have

$$ds = |\partial_u \mathbf{X}| du = |\nabla\mathcal{X}(\mathbf{Y})^\intercal \partial_u \mathbf{Y}| du = |\nabla\mathcal{X}(\mathbf{Y})^\intercal \mathbf{t}(\mathbf{Y})| |\partial_u \mathbf{Y}| du,$$

where $\mathbf{t} = \mathbf{t}(\mathbf{Y}) = \partial_u \mathbf{Y} / |\partial_u \mathbf{Y}|$ is the unit vector. Therefore, the derivative of $\mathbf{Y}$ w. r. to the arclength parameter s can be written as

$$\frac{\partial \mathbf{Y}}{\partial s} = \frac{1}{|\nabla\mathcal{X}(\mathbf{Y})^\intercal \mathbf{t}(\mathbf{Y})| |\partial_u \mathbf{Y}|} \frac{\partial \mathbf{Y}}{\partial u}.$$

Proposition 2. *A 3D closed curve $\Gamma_t = \{\mathbf{X}(s,t), s \in [0, L(\Gamma_t)]\} \subset \mathcal{M}$ evolves according to the geometric equation:*

$$\partial_t \mathbf{X} = a\partial_s^2 \mathbf{X} + \mathbf{F}(\mathbf{X}, \partial_s \mathbf{X}) + \alpha \partial_s \mathbf{X}, \quad \mathbf{X}(\cdot, 0) = \mathbf{X}_0(\cdot), \tag{11}$$

if and only if the function $\mathbf{Y}(\cdot, t) \subset \mathbb{R}^2$ is a solution to the parabolic equation:

$$\partial_t \mathbf{Y} = a\partial_s^2 \mathbf{Y} + \mathbf{G}(\mathbf{Y}, \partial_s \mathbf{Y}) + \alpha \partial_s \mathbf{Y}, \quad \mathbf{Y}(\cdot, 0) = \mathbf{Y}_0(\cdot), \tag{12}$$

where $a = a(\mathbf{X}, \partial_s \mathbf{X}) = a(\mathcal{X}(\mathbf{Y}), \nabla\mathcal{X}(\mathbf{Y})^\intercal \partial_s \mathbf{Y})$, $ds = |\partial_u \mathbf{X}| du = |\nabla \mathcal{X}(\mathbf{Y})^\intercal \mathbf{t}(\mathbf{Y})||\partial_u \mathbf{Y}| du$. The mapping $\mathbf{G}$ is defined as follows: $\mathbf{G}(\mathbf{Y}, \partial_s \mathbf{Y}) = M(\mathbf{Y}) \left[\partial_s \mathbf{Y}^\intercal \nabla^2 \mathcal{X}(\mathbf{Y}) \partial_s \mathbf{Y} + \mathbf{F}(\mathcal{X}(\mathbf{Y}), \nabla\mathcal{X}(\mathbf{Y})^\intercal \partial_s \mathbf{Y})\right]$, and the 2×3 matrix $M(\mathbf{Y})$ is the left Moore-Penrose pseudoinversion of $\nabla\mathcal{X}(\mathbf{Y})^\intercal$, i.e.

$$M(\mathbf{Y}) = (\nabla\mathcal{X}(\mathbf{Y})\nabla\mathcal{X}(\mathbf{Y})^\intercal)^{-1} \nabla\mathcal{X}(\mathbf{Y}), \tag{13}$$

and $\mathbf{X}(u,0) = \mathcal{X}(\mathbf{Y}(u,0))$, $u \in I$.

For the Moore-Penrose pseudoinversion we refer to Pavlíková [41] and references therein.

Remark 2. *As an initial condition, we can consider $\mathbf{Y}(u,0) = (ku, lu)^\intercal$, $u \in I$ where $k, l \in \mathbb{N}$ (see Figs. 1 and 2), Discretization of the initial condition is as follows:*

$$\mathbf{Y}_i(0) = \mathbf{Y}(u_i, 0), \; i = 1, \ldots, N.$$

The 2×2 matrix $\nabla\mathcal{X}(\mathbf{Y})\nabla\mathcal{X}(\mathbf{Y})^\intercal$ is positive definite because the mapping $\mathcal{X}$ is immersion. For the torus surface we have

$$det(\nabla\mathcal{X}(\mathbf{Y})\nabla\mathcal{X}(\mathbf{Y})^\intercal) = 16\pi^4 r^2 (R + r\cos(2\pi v))^2 \geq 16\pi^4 r^2 (R - r)^2 > 0.$$

On the other hand, for the Klein bottle surface shown in Fig. 2 (right) we observe large spectral variations in the 2×2 positive definite matrix $\nabla\mathcal{X}(\mathbf{Y})\nabla\mathcal{X}(\mathbf{Y})^\intercal$. Namely,

$$det(\nabla\mathcal{X}(\mathbf{Y})\nabla\mathcal{X}(\mathbf{Y})^\intercal) \in (0.0145, 32020).$$

An example of non-orientable Klein bottle immersed manifold in $\mathbb{R}^3$ parametrerized by $\mathcal{X} = (\mathcal{X}_1, \mathcal{X}_2, \mathcal{X}_3)$ where

$$\begin{aligned}
\mathcal{X}_1(u,v) &= -(2/15)\cos(2\pi u)(3\cos(2\pi v) - 30\sin(2\pi u) + 90\cos(2\pi u)^4 \sin(2\pi u) \\
&\quad -60\cos(2\pi u)^6 \sin(2\pi u) + 5\cos(2\pi u)\cos(2\pi v)\sin(2\pi u)), \\
\mathcal{X}_2(u,v) &= -(1/15)\sin(2\pi u)(3\cos(2\pi v) - 3\cos(2\pi u)^2\cos(2\pi v) - 48\cos(2\pi u)^4\cos(2\pi v) \\
&\quad +48\cos(2\pi u)^6\cos(2\pi v) + 60\sin(2\pi u) + 5\cos(2\pi u)\cos(2\pi v)\sin(2\pi u) \\
&\quad -5\cos(2\pi u)^3\cos(2\pi v)\sin(2\pi u) - 80\cos(2\pi u)^5\cos(2\pi v)\sin(2\pi u) \\
&\quad +80\cos(2\pi u)^7\cos(2\pi v)\sin(2\pi u)), \\
\mathcal{X}_3(u,v) &= (2/15)(3 + 5\cos(2\pi u)\sin(2\pi u))\sin(2\pi v).
\end{aligned}$$

The surface of the Klein bottle is shown in Fig. 2, b). The initial curve $\mathbf{X}_0$ is parameterized by

$$\mathbf{X}_0(u) = \mathcal{X}(ku, lu), \quad u \in I,$$

where $k = 1, l = 4$. It is shown in Fig. 2, a). The Klein bottle is an immersed manifold in $\mathbb{R}^3$. It is well known that it can be embedded in $\mathbb{R}^4$ but it cannot be embedded in $\mathbb{R}^3$.

4. Existence and uniqueness of classical Hölder smooth solutions

In this section, we present results on the existence and uniqueness of the classical Hölder smooth solution to the system of equations (2) for the motion of the time-dependent family of curves $\Gamma_t = \{\mathbf{X}(u,t),\ u \in I\},\ t \geq 0$, evolving in $\mathbb{R}^3$. Furthermore, we prove the existence and uniqueness of solutions $\mathbf{Y} = \mathbf{Y}(u,t)$ of the non-linear equation (12) (see Proposition 2). We employ the analytical framework developed by Beneš, Kolář, Ševčovič [6, 7] in the context of curve evolution in $\mathbb{R}^3$ and Mikula and Ševčovič [33, 34, 35, 36] for the evolution of planar curves. The proof of the existence and uniqueness of solutions in Hölder spaces is based on the abstract theory of analytic semiflows in Banach spaces, as established by DaPrato and Grisvard [19], Angenent [1, 2] and Lunardi [30]. The proof is based on the analysis of the position vector equation (2), where a uniform tangential velocity v_T is considered. The nonlinear parabolic equation (2), and similarly (12), can be rewritten as the abstract parabolic equation: $\partial_t \mathbf{X} = \mathscr{F}(\mathbf{X}),\ \mathbf{X}(0) = \mathbf{X}_0$, on a scale of suitable Banach spaces. Suppose $0 < \varepsilon < 1$, and $k \in \mathbf{N}$. The little Hölder space $h^{k+\varepsilon}(S^1)$ is the Banach space defined as the closure of C^∞ smooth functions defined in the periodic domain S^1. The norm is the sum of the C^k norm and the ε-Hölder semi-norm of the k-th derivative. Next, we define the following scale of Banach spaces consisting of $(2k+\varepsilon)$-Hölder continuous functions in the periodic domain $I \simeq S^1$:

$$\mathcal{E}_k^X = h^{2k+\varepsilon}(S^1) \times h^{2k+\varepsilon}(S^1) \times h^{2k+\varepsilon}(S^1), \quad \mathcal{E}_k^Y = h^{2k+\varepsilon}(S^1) \times h^{2k+\varepsilon}(S^1), \quad k = 0, \frac{1}{2}, 1. \tag{14}$$

For the application of the theory of nonlinear analytic semiflovs due to DaPrato and Grisvard [19], Angenent [1, 2], and Lunardi [30], it is sufficient to prove that, for any $\tilde{\mathbf{X}}$, the linearization $\mathscr{A} = \mathscr{F}'(\tilde{\mathbf{X}})$ generates an analytic semigroup in the space in $\mathcal{E}_0^Z$, and it belongs to the maximal regularity class between Banach spaces $\mathcal{E}_1^Z$ and $\mathcal{E}_0^Z$ for $Z \in \{X, Y\}$. Now we can state the following result, stating the local existence and uniqueness of solutions to the system of nonlinear geometric equations (2).

Theorem 3. *Assume $\mathscr{M} \in \mathbb{R}^3$ is an embedded manifold given by $\mathscr{M} = \{\mathbf{X} \in \mathbb{R}^3,\ f(\mathbf{X}) = 0\}$ where $f : \mathbb{R}^3 \to \mathbb{R}$ is a C^4 smooth regular map, i.e., $\nabla f(\mathbf{X}) \neq 0$ for $\mathbf{X} \in \mathscr{M}$, and $a = a(\mathbf{X}, \mathbf{T}) > 0$ is a C^2 smooth function, $a : \mathbb{R}^2 \times \mathbb{R}^2 \to \mathbb{R}$. Assume that $h : \mathbb{R} \to \mathbb{R}$ is a C^2 smooth function, $h(0) = 0$. Suppose that the parameterization $\mathbf{X}_0$ of the initial curve Γ_0 belongs to the Hölder space $\mathcal{E}_1^X$, and it is uniformly parameterized $|\partial_u \mathbf{X}_0(u)| = L(\Gamma_0) > 0$ for all $u \in I$. Assume that the total tangential velocity v_T preserves the relative local length. Then there exists $T > 0$ and the unique solution $\mathbf{X}$ to the initial value problem:*

$$\partial_t \mathbf{X} = a \partial_s^2 \mathbf{X} + \mathbf{F}(\mathbf{X}, \partial_s \mathbf{X}) + \alpha \partial_s \mathbf{X}, \quad \mathbf{X}(\cdot, 0) = \mathbf{X}_0(\cdot),\ u \in I,\ t \in [0, T),$$

where the external force $\mathbf{F}$ is given by (5). Moreover, $\mathbf{X} \in C([0,T], \mathcal{E}_1^X) \cap C^1([0,T], \mathcal{E}_0^X)$.

Proof. We rewrite the non-linear parabolic equation (2) in the form: $\partial_t \mathbf{X} = \mathscr{F}(\mathbf{X})$, where $\mathscr{F}(\mathbf{X}) = a\partial_s^2 \mathbf{X} + \mathbf{F}(\mathbf{X}, \partial_s \mathbf{X}) + \alpha \partial_s \mathbf{X}$. Under the assumptions made on functions a, f, and h, the mapping

$$\mathcal{E}_{\frac{1}{2}}^X \ni \mathbf{X} \mapsto \mathbf{F}(\mathbf{X}, \partial_s \mathbf{X}) + \alpha \partial_s \mathbf{X} \in \mathcal{E}_0^X$$

is C^1 mapping from the Banach space $\mathcal{E}_{\frac{1}{2}}^X$ to $\mathcal{E}_0^X$.

Assume $\tilde{\mathbf{X}}$ belongs to the Hölder space $\mathcal{E}_1^X$, and it is uniformly parameterized, $|\partial_u \bar{\mathbf{X}}| = L(\tilde{\Gamma}) > 0$ for all $u \in I$. Then the linearization $\mathscr{A} = \mathscr{F}'(\tilde{\mathbf{X}})$ can be decomposed as follows: $\mathscr{A} = \mathscr{A}_0 + \mathscr{A}_1$

where the principal part $\mathscr{A}_0$ containing the second order derivative has the form $\mathscr{A}_0\mathbf{X} = \frac{\tilde{a}}{L(\tilde{\Gamma})^2}\partial_u^2\mathbf{X}$. It is known that $\mathscr{A}_0$ generates an analytic semigroup in the space in $\mathcal{E}_0^X$, and it belongs to the maximal regularity class between the Banach spaces $\mathcal{E}_1^X$ and $\mathcal{E}_0^X$ (cf. [1, 2]). Furthermore, the operator $\mathscr{A}_1 = \mathscr{A} - \mathscr{A}_0$ first order derivative of $\mathbf{X}$. It is a bounded linear operator $\mathscr{A}_1 : \mathscr{E}_{\frac{1}{2}} \to \mathscr{E}_0$. Therefore, the operator $\mathscr{A}_1$ considered as a mapping from $\mathscr{E}_1 \to \mathscr{E}_0$ has the relative zero norm with respect to $\mathscr{A}_0$. Therefore, the linearization $\mathscr{A}$ belongs to the maximal regularity class $\mathcal{M}(\mathscr{E}_1, \mathscr{E}_0)$ because this class is closed with respect to perturbation with the relative zero norm (cf. [2, Lemma 2.5], DaPrato and Grisvard [19], Lunardi [30]). The proof now follows [2, Theorem 2.7] due to Angenent. $\square$

Theorem 4. *Assume $\mathscr{M}$ is an immersed manifold in $\mathbb{R}^3$ given by $\mathscr{M} = \{\mathbf{X} = \mathcal{X}(\mathbf{Y}), \quad \mathbf{Y} \in I \times I\}$ where $\mathcal{X} : I \times I \to \mathbb{R}^3$, is a C^4 smooth immersion, rank$(\nabla\mathcal{X}(\mathbf{Y})) = 2$ for all $\mathbf{Y} \in I \times I$, and $a = a(\mathbf{X}, \mathbf{T}) > 0$ is a C^2 smooth function, $a : \mathbb{R}^2 \times \mathbb{R}^2 \to \mathbb{R}$. Suppose that the initial condition $\mathbf{Y}_0$ belongs to the Hölder space $\mathcal{E}_1^Y$, and $|\partial_u \mathbf{Y}_0(u)| > 0$ for all $u \in I$. Then there exists $T > 0$ and the unique solution $\mathbf{Y}$ to the initial value problem:*

$$\partial_t \mathbf{Y} = a\partial_s^2 \mathbf{Y} + \mathbf{G}(\mathbf{Y}, \partial_s \mathbf{Y}), \quad \mathbf{Y}(\cdot, 0) = \mathbf{Y}_0(\cdot),\ u \in I,\ t \in [0, T),$$

where $\mathbf{G}(\mathbf{Y}, \partial_s\mathbf{Y}) = M(\mathbf{Y}) \left[\partial_s \mathbf{Y}^\intercal \nabla^2 \mathcal{X}(\mathbf{Y})\partial_s \mathbf{Y} + \mathbf{F}(\mathcal{X}(\mathbf{Y}), \nabla\mathcal{X}(\mathbf{Y})^\intercal \partial_s \mathbf{Y})\right]$, and the 2×3 left Moore-Penrose pseudoinversion $M(\mathbf{Y})$ is given by (13). Moreover, $\mathbf{Y} \in C([0, T], \mathcal{E}_1^Y) \cap C^1([0, T], \mathcal{E}_0^Y)$.

Proof. Under the assumptions made on the immersion mapping $\mathcal{X} : I \times I \to \mathbb{R}^3$, we have

$$\mathcal{E}_{\frac{1}{2}}^Y \ni \mathbf{Y} \mapsto \mathbf{G}(\mathbf{Y}, \partial_s \mathbf{Y}) + \alpha\partial_s \mathbf{Y} \in \mathcal{E}_0^Y$$

is a C^1 mapping from the Banach space $\mathcal{E}_{\frac{1}{2}}^Y$ to $\mathcal{E}_0^Y$. The rest of the proof is essentially the same as that of Theorem 3. $\square$

5. Flowing finite volumes numerical discretization scheme

In this section, we present a numerical discretization scheme for solving the system of equations (2), which is enhanced by adding the tangential velocity α. The discretization utilizes the method of lines with spatial discretization achieved through the finite-volume method. We focus on evolution of curves $\Gamma_t, t \geq 0$, satisfying the governing equation:

$$\partial_t \mathbf{X} = a\partial_s^2 \mathbf{X} + \mathbf{F}(\mathbf{X}, \partial_s \mathbf{X}) + \alpha \mathbf{T}. \tag{15}$$

We consider M discrete nodes $\mathbf{X}_k = \mathbf{X}(u_k)$, $k = 0, 1, 2, \ldots, M$, $\mathbf{X}_0 = \mathbf{X}_M$ along the curve Γ_t. The dual nodes are defined as $\mathbf{X}_{k\pm\frac{1}{2}} = \mathbf{X}(u_k \pm h/2)$ (see Fig. 3) where $h = 1/M$, $u_k = kh \in [0, 1]$ and $(\mathbf{X}_k + \mathbf{X}_{k+1})/2$ is the midpoint of the line segment connecting nodes $\mathbf{X}_k$ and $\mathbf{X}_{k+1}$ and differs from $\mathbf{X}_{k\pm\frac{1}{2}} \in \Gamma_t$. The k-th segment $\mathcal{S}_k$ of Γ_t between the nodes $\mathbf{X}_{k+\frac{1}{2}}$ and $\mathbf{X}_{k-\frac{1}{2}}$ represents the finite volume. Integration of equation (15) over such a volume yields

$$\int_{u_{k-\frac{1}{2}}}^{u_{k+\frac{1}{2}}} \partial_t \mathbf{X}|\partial_u \mathbf{X}|du = \int_{u_{k-\frac{1}{2}}}^{u_{k+\frac{1}{2}}} a\frac{\partial}{\partial_u}\left(\frac{\partial_u \mathbf{X}}{|\partial_u \mathbf{X}|}\right) du + \int_{u_{k-\frac{1}{2}}}^{u_{k+\frac{1}{2}}} \mathbf{F}|\partial_u \mathbf{X}|du + \int_{u_{k-\frac{1}{2}}}^{u_{k+\frac{1}{2}}} \alpha\partial_u \mathbf{X}du. \tag{16}$$

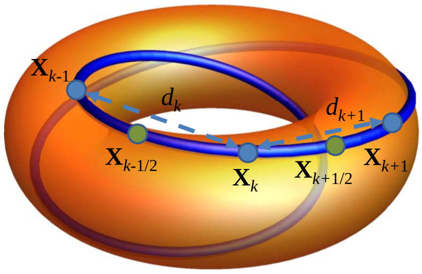

Figure 3: Discretization of a segment of a 3D curve on a surface by the method of flowing finite volumes.

Let us denote $d_k = |\mathbf{X}_k - \mathbf{X}_{k-1}|$ for $k = 1, 2, \ldots, M, M+1$, where $\mathbf{X}_M = \mathbf{X}_0$ and $\mathbf{X}_{M+1} = \mathbf{X}_1$ for the closed curve Γ and we approximate the integral expressions in (16) by means of the flowing finite volume method as follows:

$$\int_{u_{k-\frac{1}{2}}}^{u_{k+\frac{1}{2}}} \partial_t \mathbf{X} |\partial_u \mathbf{X}| du \approx \frac{d\mathbf{X}_k}{dt} \frac{d_{k+1}+d_k}{2}, \qquad \int_{u_{k-\frac{1}{2}}}^{u_{k+\frac{1}{2}}} a \partial_u \frac{\partial_u \mathbf{X}}{|\partial_u \mathbf{X}|} du \approx a_k \left(\frac{\mathbf{X}_{k+1}-\mathbf{X}_k}{d_{k+1}} - \frac{\mathbf{X}_k - \mathbf{X}_{k-1}}{d_k} \right),$$
$$\int_{u_{k-\frac{1}{2}}}^{u_{k+\frac{1}{2}}} \mathbf{F} |\partial_u \mathbf{X}| du \approx \mathbf{F}_k \frac{d_{k+1}+d_k}{2}, \qquad \int_{u_{k-\frac{1}{2}}}^{u_{k+\frac{1}{2}}} \alpha \partial_u \mathbf{X} du \approx \alpha_k \frac{\mathbf{X}_{k+1}-\mathbf{X}_{k-1}}{2}.$$

The estimation of the nonnegative curvature κ along with the tangent vector $\mathbf{T}$ and the normal vector $\mathbf{N}$, where $\kappa \mathbf{N} = \partial_s \mathbf{T}$, can be expressed as follows:

$$\mathbf{N}_k \approx \frac{1}{\delta + \kappa_k} \frac{2}{d_k + d_{k+1}} \left(\frac{\mathbf{X}_{k+1}-\mathbf{X}_k}{d_{k+1}} - \frac{\mathbf{X}_k - \mathbf{X}_{k-1}}{d_k} \right), \qquad \mathbf{T}_k \approx \frac{\mathbf{X}_{k+1}-\mathbf{X}_{k-1}}{d_{k+1}+d_k},$$
$$\kappa_k \approx \left| \frac{2}{d_k + d_{k+1}} \left(\frac{\mathbf{X}_{k+1}-\mathbf{X}_k}{d_{k+1}} - \frac{\mathbf{X}_k - \mathbf{X}_{k-1}}{d_k} \right) \right|,$$

where $0 < \delta \ll 1$ is a small regularization parameter. To discretize the governing system of equations, we assume that $\partial_t \mathbf{X}, \partial_u \mathbf{X}, \mathbf{F}, \alpha, \kappa, a, b, \mathbf{T}$, and $\mathbf{N}$ remain constant on the finite volume $\mathcal{S}_k$ bounded by the nodes $\mathbf{X}_{k-\frac{1}{2}}$ and $\mathbf{X}_{k+\frac{1}{2}}$. These variables assume the values $\partial_t \mathbf{X}_k, \partial_u \mathbf{X}_k, \mathbf{F}_k, \alpha_k, \kappa_k, \mathbf{T}_k$, and $\mathbf{N}_k$, respectively. In the approximation of the nonlocal vector function $\mathbf{F}_k$, the curve Γ_t used to define $\mathbf{F}$ is replaced by a polygonal curve having vertices at $(\mathbf{X}_0, \mathbf{X}_1, \ldots, \mathbf{X}_M)$. The numerical approximation of the tangential velocity α_k is summarized at the end of this section. The semidiscrete scheme for resolving (15) is expressed as follows.

$$\begin{aligned} \frac{d\mathbf{X}_k}{dt} &= a_k \frac{2}{d_{k+1}+d_k} \left(\frac{\mathbf{X}_{k+1}-\mathbf{X}_k}{d_{k+1}} - \frac{\mathbf{X}_k - \mathbf{X}_{k-1}}{d_k} \right) + \mathbf{F}_k + \alpha_k \frac{\mathbf{X}_{k+1}-\mathbf{X}_{k-1}}{d_{k+1}+d_k}, \\ \mathbf{X}_k(0) &= \mathbf{X}_{ini}(u_k), \quad \text{for } k = 1, \ldots, M. \end{aligned}$$

The resulting system of ODEs is numerically solved using the 4th-order explicit Runge-Kutta-Merson method, incorporating automatic time step control with a tolerance level of 10^{-3} (refer to [40]). The initial time step was selected as $4h^2$, where $h = 1/M$ denotes the spatial mesh size.

Recall that the tangential component α of the velocity vector for evolving closed curves $\{\Gamma_t, t \geq 0\}$ maintains their shape unchanged (cf. Epstein and Gage [13]). However, for numerically solving

(15), the careful selection of the tangential velocity functional α is key to preserve the stability of the computational procedure (cf. in Mikula and Ševčovič [33, 34, 35]). The significance of tangential velocity is substantial in both theoretical and computational analyses of curve evolution, as shown by the works of Hou et al. [23], Kimura [26], and Mikula and Ševčovič [33, 34, 35], together with Yazaki and Ševčovič [44]. Barrett et al.[3, 4], and Elliott and Fritz [31], explored gradient and elastic flows for closed and open curves in $\mathbb{R}^d$, where $d \geq 2$, and formulated a numerical approximation method to effectively redistribute the tangential component. Furthermore, the relevance of tangential velocity is recognized in material science investigations by Beneš, Kolář, and Ševčovič [5] and in the contexts of interactive evolving curves [6]. In a different field, Garcke, Kohsaka, and Ševčovič [16] applied uniform tangential redistribution to theoretically confirm the nonlinear stability of curvature-induced flows with triple junctions in planes. Remešíková *et al.* [32] analyzed the tangential redistribution effects for the flows of the closed manifolds in $\mathbb{R}^n$. By adjusting the timing of the local relative length $|\partial_u \mathbf{X}(u,t)|$ and the total curve length $L(\Gamma_t) = \int_0^1 |\partial_u \mathbf{X}(u,t)| du$, it is possible to derive equation for the ratio:

$$\frac{\partial}{\partial t}\frac{|\partial_u \mathbf{X}(u,t)|}{L(\Gamma_t)} = \frac{|\partial_u \mathbf{X}(u,t)|}{L(\Gamma_t)}\left(\partial_s\alpha - \kappa v_N + \langle \kappa v_N\rangle\right), \quad \text{where } \langle \kappa v_N\rangle = \frac{1}{L(\Gamma)}\int_\Gamma \kappa v_N ds. \tag{17}$$

Therefore, the ratio $|\partial_u \mathbf{X}(u,t)|/L(\Gamma_t)$ is constant with respect to the time t, i.e.

$$\frac{|\partial_u \mathbf{X}(u,t)|}{L(\Gamma_t)} = \frac{|\partial_u \mathbf{X}(u,0)|}{L(\Gamma_0)}, \quad \text{for any } t \geq 0, \tag{18}$$

provided that the tangential velocity satisfies $\partial_s\alpha = \kappa v_N - \langle \kappa v_N\rangle$. Another suitable choice of the tangential velocity α is the so-called asymptotically uniform tangential velocity proposed and analyzed by Mikula and Ševčovič in [34, 35]. If the parameter $\omega > 0$ and

$$\partial_s\alpha = \kappa v_N - \langle \kappa v_N\rangle + \left(\frac{L(\Gamma_t)}{|\partial_u \mathbf{X}(u,t)|} - 1\right)\omega, \tag{19}$$

then, using (17) we obtain $\lim_{t\to\infty} \frac{|\partial_u \mathbf{X}(u,t)|}{L(\Gamma_t)} = 1$ uniformly with respect to $u \in [0,1]$ provided that $\omega > 0$ is a positive constant. This means that the redistribution becomes asymptotically uniform. The numerical approximation of the tangential velocity (19) follows from [43, 44]. It requires discrete values of curvature κ_k, normal velocity $v_{N,k}$, and segment lengths d_k, and a straightforward trapezoidal integration is used (cf. [44]). The values $\alpha_0 = \alpha_M$ are chosen such that $\sum_{i=1}^M \alpha_i(d_{i+1} + d_i)/2 = 0$. Then the values α_k for $k = 0, 1, \ldots, M$ are uniquely given and direct integration of (19) leads to the following formulas

$$\begin{aligned} \alpha_i &= \alpha_1 + \sum_{k=2}^{i}\left[\kappa_i v_{N,i} d_i - \langle \kappa v_N\rangle d_i + \left(\frac{L(\Gamma_t)}{M} - d_i\right)\omega\right], \quad i = 2,\ldots,M, \\ \alpha_1 &= -\frac{1}{\sum_{i=1}^M \frac{(d_{i+1}+d_i)}{2}}\left\{\sum_{i=2}^{M}\frac{(d_{i+1}+d_i)}{2}\left(\sum_{k=2}^{i}\left[\kappa_i v_{N,i} d_i - \langle \kappa v_N\rangle d_i + \left(\frac{L(\Gamma_t)}{M} - d_i\right)\omega\right]\right)\right\}. \end{aligned} \tag{20}$$

Remark 3. *Numerical approximation of the immersed manifold projection (12).*

$$\frac{|\mathbf{Y}_{k+1} - \mathbf{Y}_k| + |\mathbf{Y}_k - \mathbf{Y}_{k-1}|}{2}\partial_s^2 \mathbf{Y}_k \approx \int_{u_{k-\frac{1}{2}}}^{u_{k+\frac{1}{2}}} \frac{1}{|\nabla\mathcal{X}(\mathbf{Y})^\intercal \mathbf{t}(\mathbf{Y})|}\frac{\partial}{\partial u}\left(\frac{1}{|\nabla\mathcal{X}(\mathbf{Y})^\intercal \mathbf{t}(\mathbf{Y})|}\frac{\partial_u \mathbf{Y}}{|\partial_u \mathbf{Y}|}\right) du$$

$$\approx \frac{1}{|\nabla\mathcal{X}(\mathbf{Y}_k)^\intercal \mathbf{t}(\mathbf{Y}_k)|}\left(\frac{1}{|\nabla\mathcal{X}(\mathbf{Y}_{k+1})^\intercal \mathbf{t}(\mathbf{Y}_{k+1})|}\frac{\mathbf{Y}_{k+1} - \mathbf{Y}_k}{|\mathbf{Y}_{k+1} - \mathbf{Y}_k|} - \frac{1}{|\nabla\mathcal{X}(\mathbf{Y}_k)^\intercal \mathbf{t}(\mathbf{Y}_k)|}\frac{\mathbf{Y}_k - \mathbf{Y}_{k-1}}{|\mathbf{Y}_k - \mathbf{Y}_{k-1}|}\right)$$

where $\mathbf{t}(\mathbf{Y}_k) \approx (\mathbf{Y}_k - \mathbf{Y}_{k-1})/|\mathbf{Y}_k - \mathbf{Y}_{k-1}|$. *Similarly, the terms* $\partial_s \mathbf{Y}$ *and* $\partial_t \mathbf{Y}$ *in (12) can be approximated as follows:*

$$\partial_s \mathbf{Y}_k = \frac{1}{|\nabla\mathcal{X}(\mathbf{Y}_k)^\intercal \mathbf{t}(\mathbf{Y}_k)|}\partial_r \mathbf{Y}_k \approx \frac{1}{|\nabla\mathcal{X}(\mathbf{Y}_k)^\intercal \mathbf{t}(\mathbf{Y}_k)|}\frac{\mathbf{Y}_k - \mathbf{Y}_{k-1}}{|\mathbf{Y}_k - \mathbf{Y}_{k-1}|},$$

$$\int_{u_{k-\frac{1}{2}}}^{u_{k+\frac{1}{2}}} \partial_t \mathbf{Y}|\partial_u \mathbf{Y}|du \approx \frac{d\mathbf{Y}_k}{dt}\frac{d_{k+1}+d_k}{2}.$$

The approximation of the 2×3 *matrix* $M(\mathbf{Y}_k)$ *is straightforward. We approximate the partial derivatives* $\frac{\partial \mathcal{X}_i}{\partial Y_j}, i = 1,2,3, j = 1,2,$ *by meanf of finite diferences. The* 2×2 *matrix* $\nabla\mathcal{X}(\mathbf{Y})\nabla\mathcal{X}(\mathbf{Y})^\intercal$ *can be explicitly inverted. Notice that this matrix is regular because* $\mathcal{X}$ *is immersion.*

6. Examples

In our examples we consider evolution of an initial Fourier curve parameterized by a finite trigonometric series in the parameter $u \in I$. Here we remind I is identified with the unit circle and $I = \mathbb{R}/\mathbb{Z} \simeq S^1$.

In all of our numerical experiments, we use $M = 200$ discretization nodes, uniform tangential redistribution, and the regularization parameter δ in the discrete approximation of curvature was set to $\delta = 10^{-5}$.

6.1. Evolution of knotted curves on torus

As an example of a torus, we can consider immersion $\mathcal{X} : I \times I \to \mathbb{R}^3$ defined as:

$$\mathcal{X}(u,v) = \left((r\cos(2\pi v)+R)\sin(2\pi u),\ (r\cos(2\pi v)+R)\cos(2\pi u),\ r\sin(2\pi v)\right)^\intercal, \tag{21}$$

where $0 < r < R$ and $u, v \in I$. The torus surface can also be defined as an embedded manifold $\mathscr{M} = \{\mathbf{X} = (X_1, X_2, X_3)^\intercal \in \mathbb{R}^3,\ f(\mathbf{X}) = 0\}$ where

$$f(\mathbf{X}) = ((X_1^2 + X_2^2)^{\frac{1}{2}} - R)^2 + X_3^2 - r^2.$$

Its gradient $\nabla f(\mathbf{X})$ and the Hess matrix $\nabla^2 f(\mathbf{X})$ are given by

$$\nabla f(\mathbf{X}) = 2\mathbf{X} - 2R\left(X_1/(X_1^2+X_2^2)^{\frac{1}{2}},\ X_2/(X_1^2+X_2^2)^{\frac{1}{2}},\ 0\right)^\intercal, \tag{22}$$

$$|\nabla f(\mathbf{X})| = 2\left(X_1^2+X_2^2+X_3^2 - 2R(X_1^2+X_2^2)^{\frac{1}{2}} + R^2\right)^{\frac{1}{2}}, \tag{23}$$

$$\nabla^2 f(\mathbf{X}) = 2\mathbf{I} - 2\frac{R}{(X_1^2+X_2^2)^{\frac{3}{2}}}(X_2,-X_1,0)(X_2,-X_1,0)^\intercal, \tag{24}$$

$$\mathbf{T}^\intercal \nabla^2 f(\mathbf{X})\mathbf{T} = 2 - 2\frac{R}{(X_1^2+X_2^2)^{\frac{3}{2}}}(T_1X_2 - T_2X_1)^2, \tag{25}$$

where the unit tangent vector $\mathbf{T} = (T_1, T_2, T_3)^\intercal$. The torus surface is shown in Fig. 1. The initial curve $\mathbf{X}_0$ derived from mapping (21) is parameterized by

$$\mathbf{X}_0(u) = \mathcal{X}(ku, lu), \quad u \in I,$$

where $k = 2, l = 3,$ $r = 1$ and $R = 4$. Its time evolution is shown in Fig. 4. The curve shrinks and converges to the stationary state with constant length as suggested in Fig. 6 a).

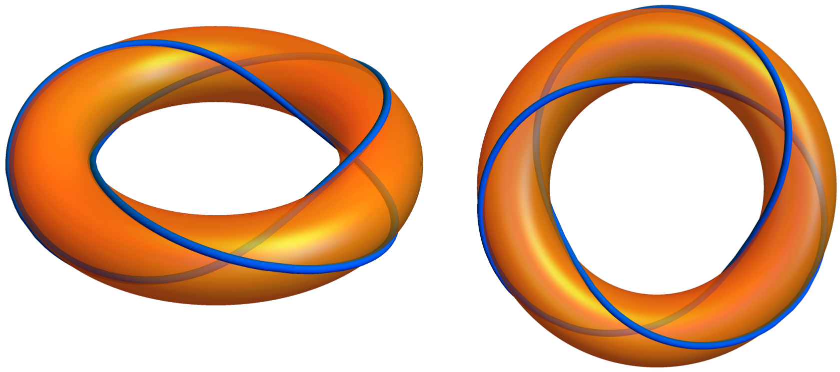

Initial curve $t = 0$

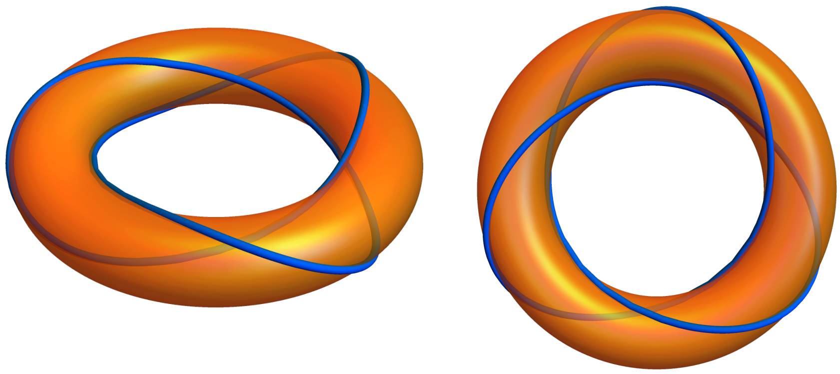

Intermmediate curve $t = 2.5$

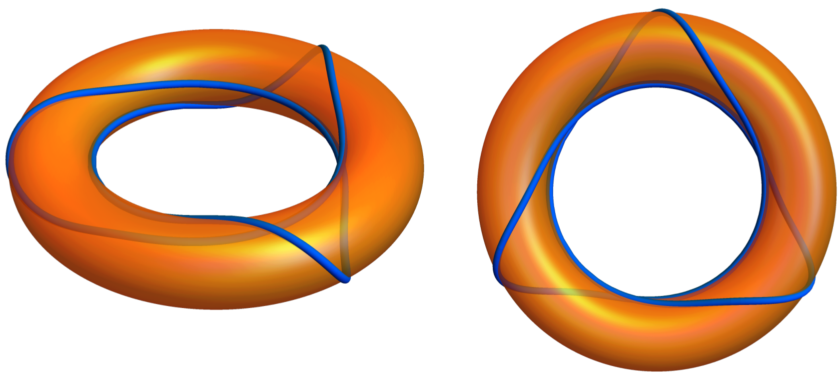

Limiting stationary curve $t = 22.5$

Figure 4: A time evolution of a knotted Fourier curve belonging to the orientable torus surface with parameters $0 < r = 1 < R = 4$, and $k = 2$, $l = 3$.

6.2. Attraction of curves by a torus surface

In this part, we present an example of evolution of initial closed curves belonging to a small neighborhood of the given surface $\mathcal{M}$ (see Proposition 1).

The following computational example demonstrates how an initially knotted curve evolves according to geometric evolution equation (2) driven by the force term (5). The reference surface is the torus given by immersion (21) with $r = 1$, $R = 4$. The initial curve $\mathbf{X}_0$ is parametrized by mapping (21) as

$$\mathbf{X}_0(u) = \mathcal{X}(ku, lu), \quad u \in I,$$

where $k = 3, l = 5$, $r = 2$ and $R = 4$. The time evolution of such an inflated initial curve is shown in Fig. 5. The curve continues to shrink until it attaches to the torus surface and eventually finds its stationary state with constant length, as suggested in Fig. 6 b).

6.3. Evolution of simple curves on surface with genius 0 with humps

The last example is shown in Fig. 7. $\mathscr{M} = \{\mathbf{X} = (X_1, X_2, X_3)^\intercal \in \mathbb{R}^3,\ f(\mathbf{X}) = 0\}$ where

$$f(\mathbf{X}) = X_1^2 + X_2^2 + c^2(X_3 - \phi(X_1, X_2))^2 - r^2, \quad \phi(X_1, X_2) = h(X_1 - 1, X_2) + h(X_1 + 1, X_2),$$

where h is a smooth bump function, $h(X_1, X_2) = v\, 2^{-1/(1-X_1^2-X_2^2)}$ for $X_1^2+X_2^2 < 1$, and $h(X_1, X_2) = 0$, otherwise. In the example shown in Fig. 7 we set $r = 2.5, c = 4$, and $v = 3$. The initial curve is an ellipse projected onto the surface, i.e.

$$\Gamma_0 = \{\mathbf{X} = (X_1, X_2, X_3), \quad X_1^2/2 + X_2^2 = 2, \quad X_3 = c^{-1}(r^2 - X_1^2 - X_2^2)^{\frac{1}{2}} + \phi(X_1, X_2).$$

7. Conclusion

In this paper, we investigated the curvature-driven flow of a family of closed curves evolving on an embedded or immersed manifold in the three-dimensional Euclidean space. We analyzed the qualitative behavior of such a flow. Using the abstract theory of analytic semi-flows in Banach spaces, we prove the local existence and uniqueness of Hölder smooth solutions to the governing system of evolution equations for the curve parametrization. We demonstrate the behavior of sulutions in several computational examples constructed by means of the flowing finite-volume method and asymptotically uniform tangential redistribution of discretization points.

Declarations

Funding: D. Ševčovič was supported by the VEGA 1-0493-24 research project. M. Kolář was supported by Czech Science Foundation Project no. 25-18265S - Computational models of hydraulic fracturing in geothermal energy production.
Conflict of interest: The authors declares that there are no conflicts of interest regarding the publication of this paper
Author Contributions: The authors contributed equally to the study.
Ethical approval: Not applicable.
Data availability: All data in this paper are available from the author on a reasonable request.

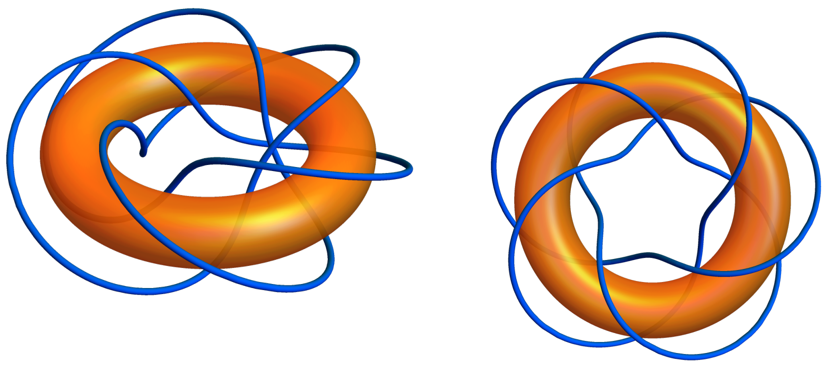

Initial curve $t = 0$

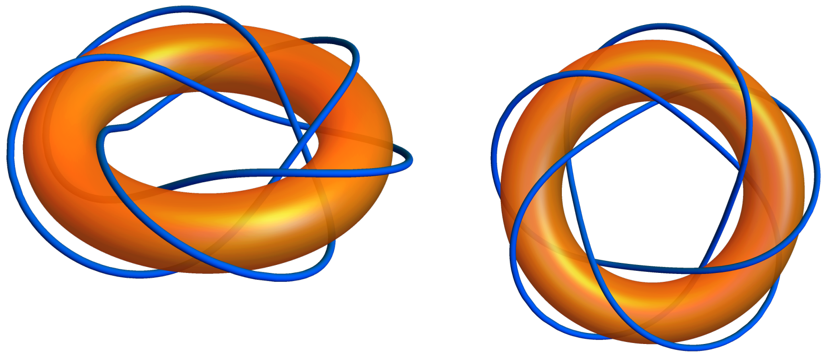

Intermmediate curve $t = 1$

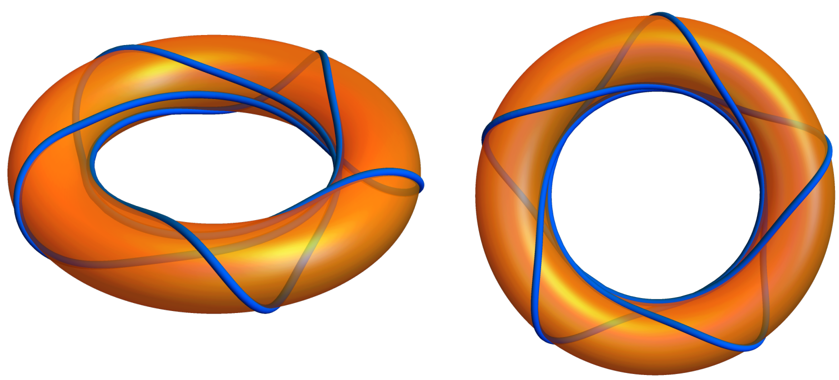

Limiting stationary curve $t = 19.75$

Figure 5: A time evolution of initially inflated knotted curve belonging to the orientable torus surface with parameters $0 < r = 1 < R = 4$. Topologically more complex case corresponding to the choice $k = 3$, $l = 5$ in initial condition.

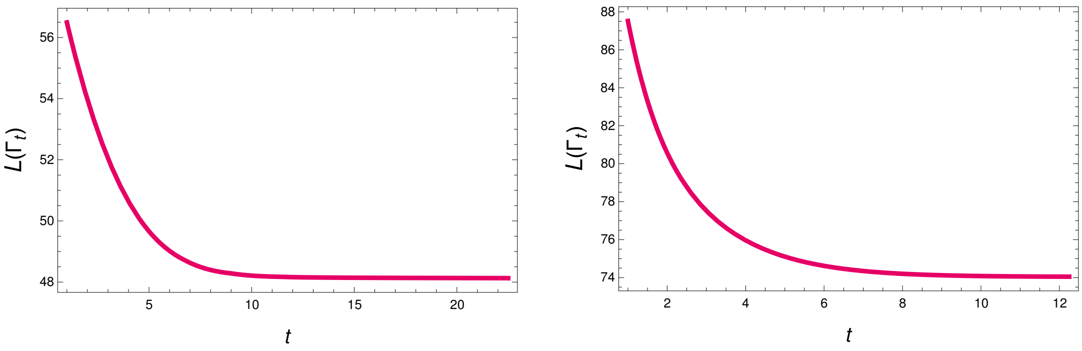

a) b)

Figure 6: Lengths $L(\Gamma_t)$ of shrinking curves on the torus (21) - a) and attaching to the torus (21) - b).

References

[1] S. Angenent, *Parabolic equations for curves on surfaces part i. curves with p-integrable curvature*, Annals of Mathematics, (1990), pp. 451–483.

[2] S. B. Angenent, *Nonlinear analytic semiflows*, Proceedings of the Royal Society of Edinburgh Section A: Mathematics, 115 (1990), pp. 91–107.

[3] J. W. Barrett, H. Garcke, and R. Nürnberg, *Numerical approximation of gradient flows for closed curves in R^d*, IMA journal of numerical analysis, 30 (2010), pp. 4–60.

[4] ———, *Parametric approximation of isotropic and anisotropic elastic flow for closed and open curves*, Numerische Mathematik, 120 (2012), pp. 489–542.

[5] M. Beneš, M. Kolář, and D. Ševčovič, *Area preserving geodesic curvature driven flow of closed curves on a surface*, Discrete Contin. Dyn. Syst. Ser. B, 22 (2017), pp. 3671–3689.

[6] ———, *Curvature driven flow of a family of interacting curves with applications*, Mathematical Methods in the Applied Sciences, 43 (2020), pp. 4177–4190.

[7] ———, *Qualitative and numerical aspects of a motion of a family of interacting curves in space*, SIAM journal on applied mathematics, 82 (2022), pp. 549–575.

[8] ———, *On diffusion and transport acting on parameterized moving closed curves in space*, arXiv preprint arXiv:2404.02260, (2024).

[9] T. Binz and B. Kovács, *A convergent finite element algorithm for mean curvature flow in arbitrary codimension*, Interfaces and Free Boundaries, 25 (2023), pp. 373–400.

[10] K. Deckelnick, *Weak solutions of the curve shortening flow*, Calculus of Variations and Partial Differential Equations, 5 (1997), pp. 489–510.

[11] K. Deckelnick and R. Nürnberg, *Discrete anisotropic curve shortening flow in higher codimension*, IMA Journal of Numerical Analysis, 45 (2025), pp. 36–67.

[12] G. Dziuk, *Convergence of a semi-discrete scheme for the curve shortening flow*, Mathematical Models and Methods in Applied Sciences, 4 (1994), pp. 589–606.

[13] C. Epstein and M. Gage, *The curve shortening flow*, in Wave Motion: Theory, Modelling, and Computation: Proceedings of a Conference in Honor of the 60th Birthday of Peter D. Lax, Springer, 1987, pp. 15–59.

[14] J. Fierling, A. Johner, I. M. Kulić, H. Mohrbach, and M. M. Müller, *How bio-filaments twist membranes*, Soft Matter, 12 (2016), pp. 5747–5757.

[15] M. Gage and R. S. Hamilton, *The heat equation shrinking convex plane curves*, Journal of Differential Geometry, 23 (1986), pp. 69–96.

[16] H. Garcke, Y. Kohsaka, and D. Ševčovič, *Nonlinear stability of stationary solutions for curvature flow with triple junction*, Hokkaido Mathematical Journal, 38 (2009), pp. 721–769.

[17] C. M. Gilmore, *Fundamentals and applications of micro-and nanofibers*, MRS BULLETIN, 40 (2015), pp. 87–88.

[18] M. Glagolev and V. Vasilevskaya, *Liquid-crystalline ordering of filaments formed by bidisperse amphiphilic macromolecules*, Polymer Science, Series C, 60 (2018), pp. 39–47.

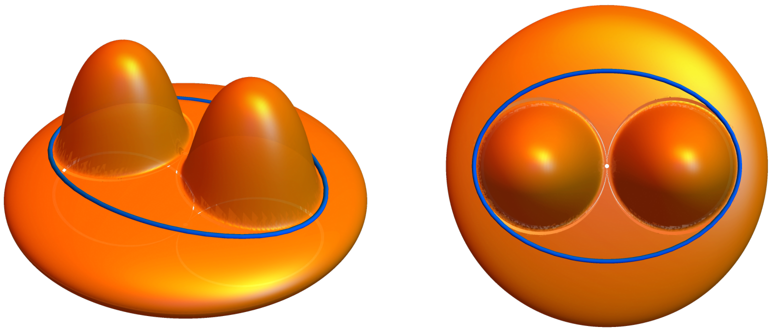

Initial curve $t = 0$

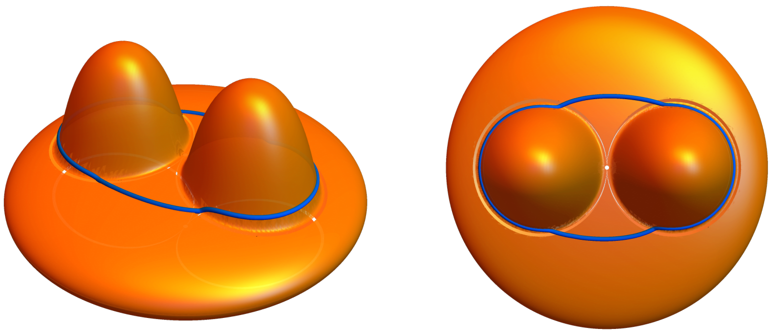

Intermmediate curve $t = 4.5$

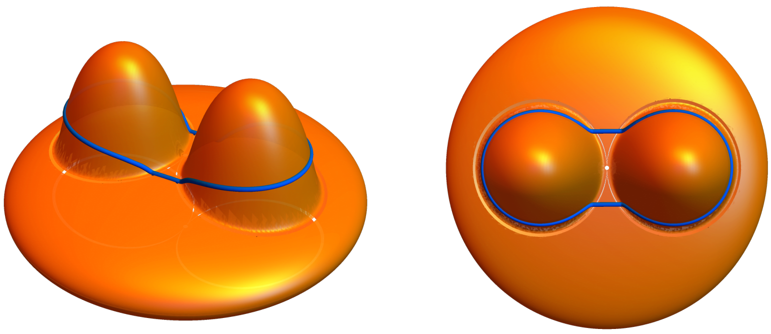

Limiting stationary curve $t = 13.5$

Figure 7: Evolution of a simple curve belonging to the orientable surface of genus 0 with humps.

[19] G. D. P.-P. Grisvard and G. Da Prato, *Equations d'évolution abstraites non linéaires de type parabolique*, Ann. Mat. Pura Appl.,(4), 120 (1979), pp. 329–396.

[20] J.-H. He, Y. Liu, L.-F. Mo, Y.-Q. Wan, and L. Xu, *Electrospun nanofibres and their applications*, ISmithers Shawbury, UK, 2008.

[21] H. Helmholtz, *Über Integrale der hydrodynamischen Gleichungen, welche den Wirbelbewegungen entsprechen.*, J. Reine Angew. Math., 55 (1858), pp. 25–55.

[22] D. Henry, *Geometric theory of semilinear parabolic equations*, vol. 840, Springer, 2006.

[23] T. Y. Hou, J. S. Lowengrub, and M. J. Shelley, *Removing the stiffness from interfacial flows with surface tension*, Journal of Computational Physics, 114 (1994), pp. 312–338.

[24] M. Kang, H. Cui, and S. M. Loverde, *Coarse-grained molecular dynamics studies of the structure and stability of peptide-based drug amphiphile filaments*, Soft Matter, 13 (2017), pp. 7721–7730.

[25] T. Kemmochi, Y. Miyatake, and K. Sakakibara, *Structure-preserving numerical methods for constrained gradient flows of planar closed curves with explicit tangential velocities*, Japan Journal of Industrial and Applied Mathematics, (2024), pp. 1–29.

[26] M. Kimura, *Numerical analysis of moving boundary problems using the boundary tracking method*, Japan journal of industrial and applied mathematics, 14 (1997), pp. 373–398.

[27] M. Kolár, M. Beneš, and D. Ševcovic, *Area preserving geodesic curvature driven flow of closed curves on a surface*, Discrete Contin. Dyn. Syst. Ser. B, 22 (2017), pp. 3671–3689.

[28] M. Kolář, P. Pauš, J. Kratochvíl, and M. Beneš, *Improving method for deterministic treatment of double cross-slip in fcc metals under low homologous temperatures*, Computational Materials Science, 189 (2021), p. 110251.

[29] M. Kolář and D. Ševčovič, *Evolution of multiple closed knotted curves in space*, Proceedings of the Conference Algoritmy, (2024), pp. 129–138.

[30] A. Lunardi, *Abstract quasilinear parabolic equations*, Mathematische Annalen, 267 (1984), pp. 395–415.

[31] C. M. Elliott and H. Fritz, *On approximations of the curve shortening flow and of the mean curvature flow based on the deturck trick*, IMA Journal of Numerical Analysis, 37 (2017), pp. 543–603.

[32] K. Mikula, M. Remešíková, P. Sarkoci, and D. Ševčovič, *Manifold evolution with tangential redistribution of points*, SIAM Journal on Scientific Computing, 36 (2014), pp. A1384–A1414.

[33] K. Mikula and D. Ševčovič, *Evolution of plane curves driven by a nonlinear function of curvature and anisotropy*, SIAM Journal on Applied Mathematics, 61 (2001), pp. 1473–1501.

[34] ———, *Computational and qualitative aspects of evolution of curves driven by curvature and external force*, Computing and Visualization in Science, 6 (2004), pp. 211–225.

[35] ———, *A direct method for solving an anisotropic mean curvature flow of plane curves with an external force*, Mathematical Methods in the Applied Sciences, 27 (2004), pp. 1545–1565.

[36] ———, *Evolution of curves on a surface driven by the geodesic curvature and external force*, Applicable Analysis, 85 (2006), pp. 345–362.

[37] M. Narayanan and M. Beneš, *Evolution of space curves by parametric method with natural and uniform redistribution*, Proceedings of the Conference Algoritmy, (2024), pp. 109–118.

[38] X. Niu, Y. Gu, and Y. Xiang, *Dislocation dynamics formulation for self-climb of dislocation loops by vacancy pipe diffusion*, International Journal of Plasticity, 120 (2019), pp. 262–277.

[39] X. Niu, T. Luo, J. Lu, and Y. Xiang, *Dislocation climb models from atomistic scheme to dislocation dynamics*, Journal of the Mechanics and Physics of Solids, 99 (2017), pp. 242–258.

[40] P. Pauš, M. Beneš, M. Kolář, and J. Kratochvíl, *Dynamics of dislocations described as evolving curves interacting with obstacles*, Modelling and Simulation in Materials Science and Engineering, 24 (2016), p. 035003.

[41] S. Pavlíková and D. Ševčovič, *On the Moore-Penrose pseudo-inversion of block symmetric matrices and its application in the graph theory*, Linear Algebra and its Applications, 673 (2023), pp. 280–303.

[42] D. H. Reneker and A. L. Yarin, *Electrospinning jets and polymer nanofibers*, Polymer, 49 (2008), pp. 2387–2425.

[43] D. Ševčovič and S. Yazaki, *Evolution of plane curves with a curvature adjusted tangential velocity*, Japan journal of industrial and applied mathematics, 28 (2011), pp. 413–442.

[44] ———, *Computational and qualitative aspects of motion of plane curves with a curvature adjusted tangential velocity*, Mathematical Methods in the Applied Sciences, 35 (2012), pp. 1784–1798.

[45] R. Shlomovitz and N. Gov, *Membrane-mediated interactions drive the condensation and coalescence of ftsz rings*, Physical biology, 6 (2009), p. 046017.

[46] R. Shlomovitz, N. Gov, and A. Roux, *Membrane-mediated interactions and the dynamics of dynamin oligomers on membrane tubes*, New Journal of Physics, 13 (2011), p. 065008.

[47] L. Xu, H. Liu, N. Si, and E. Wai Ming Lee, *Numerical simulation of a two-phase flow in the electrospinning process*, International Journal of Numerical Methods for Heat & Fluid Flow, 24 (2014), pp. 1755–1761.